THE JOURNAL OF PHYSICAL CHEMISTRY B

Article

Ionic Surfactant Aggregates in Saline Solutions: Sodium Dodecyl Sulfate (SDS) in the Presence of Excess Sodium Chloride (NaCl) or Calcium Chloride (CaCl)

Maria Sammalkorpi, Mikko Karttunen, and Mikko Haataja

J. Phys. Chem. B, **2009**, 113 (17), 5863-5870• DOI: 10.1021/jp901228v • Publication Date (Web): 03 April 2009

Ionic Surfactant Aggregates in Saline Solutions: Sodium Dodecyl Sulfate (SDS) in the Presence of Excess Sodium Chloride (NaCl) or Calcium Chloride ($CaCl_2$)

Maria Sammalkorpi,*,† Mikko Karttunen,‡ and Mikko Haataja†

Department of Mechanical and Aerospace Engineering, Princeton University, Princeton, New Jersey 08544, and Department of Applied Mathematics, The University of Western Ontario, London, Ontario, Canada N6A 5B7

Received: February 10, 2009; Revised Manuscript Received: March 2, 2009

The properties of sodium dodecyl sulfate (SDS) aggregates in saline solutions of excess sodium chloride (NaCl) or calcium chloride ($CaCl_2$) ions were studied through extensive molecular dynamics simulations with explicit solvent. We find that the ionic strength of the solution affects not only the aggregate size of the resulting anionic micelles but also their structure. Specifically, the presence of $CaCl_2$ induces more compact and densely packed micelles with a significant reduction in *gauche* defects in the SDS hydrocarbon chains in comparison with NaCl. Furthermore, we observe significantly more stable salt bridges between the charged SDS head groups mediated by Ca^{2+} than Na^+. The presence of these salt bridges helps stabilize the more densely packed micelles.

1. Introduction

Micellization is a self-assembly phenomenon that occurs in solutions of amphiphilic molecules (surfactants), proteins, peptides, and block copolymers.[1] In aqueous solutions above the critical micellization concentration, surfactants form insoluble crystals or micelles depending on temperature.[2,3] More complex phases, such as cubic or lamellar, may also occur.[1,3−7] These self-assembling structures appear across a broad range of length scales[8] and can be exploited in a myriad of applications, such as nanocarriers in drug delivery,[9,10] emulsions and foams,[11] and even nanolithography.[1] Interestingly, in the case of ionic surfactants, the concentration and type of excess salt provides another means to control the aggregate structure and properties.

A fundamental understanding of the physical mechanisms which control self-assembly processes requires detailed, microscopic level molecular information. Experimentally, extracting this information is very challenging due to the characteristic length (∼20 nm) and time (∼1 μs) scales associated with surfactant micelles. One of the most important issues is electrostatics as many molecules become ionized in aqueous solutions, and ions and the ionic strength of the solution largely control the association and dissociation of molecules in micelles.[12−18] While it is tempting to subsume the excess salt degrees of freedom into an effective screened interaction between the charged surfactants, it has been very recently demonstrated that such a mean-field picture does not quantitatively capture the effect of excess salt on aggregate structure in thermal equilibrium.[19] In this work, we examine the role of electrostatic interactions and the presence of excess salt on both aggregate structure and dynamics by employing molecular dynamics simulations with explicit solvent and salt.

Molecular dynamics (MD) simulations provide a natural method to study the interactions and the kinetic pathways of self-assembly processes when the time and length scales are not too large. Thus far, micellization has been studied mostly by lattice and off-lattice coarse-grained models.[20−28] More recently, atomistic studies with and without solvent have emerged.[29−39] Since characteristic equilibration times for micelle formation are on the order of microseconds or longer, most of these simulations start from a spherical or rodlike micelle with a predetermined number of detergent molecules.[26,30,33,35,36,40] Such an approach provides valuable insight into detergent dynamics and micelle structure within that particular initial setup, but the results implicitly contain the assumption that the global minimum energy configuration, that is, micellar shape and aggregation number, is close to the initial configuration. Although computationally much more demanding, a random initial configuration is a more natural approach as it relaxes the above limitations. Marrink et al.[32] studied the micellization of 54 dodecylphosphocholine (DPC) molecules and reported a concentration-dependent aggregate structure. In our previous work we provided analyses of the temperature dependence of sodium dodecyl sulfate (SDS) micellization through extensive (200 ns) MD simulations with atomistic detail and also saw concentration dependence and evidence of rodlike micelles.[37,38] Lazaridis et al.[39] simulated 960 DPC molecules in an implicit environment providing to date the temporally most extensive micellization data but without explicit solvent. Very recently, models that combine atomistic simulations and a thermodynamic approach for micelle formation[41] have emerged.

In this study, we focus on the effects of sodium chloride and calcium chloride on micellar systems consisting of SDS. SDS is the archetypal and the most commonly used ionic surfactant. Its use in biochemistry dates back, at least, to the 1940s.[42] Seminal work on its structure and phase behavior was performed by Cabane, Kékicheff, and co-workers in a series of papers in the middle of the 1980s in which they established the importance of fluctuations and that the pathway from a planar system to rodlike micelles occurs through several intermediate morphologies.[4,5,43,44] The effects of ionic concentration on micelle formation have been of keen interest for more than 40 years, see, e.g., refs 14, 15, and 45−51, and ionic strength of the solution has been demonstrated as a means to tailor the

* Corresponding author. E-mail: msammalk@princeton.edu. Formerly M. Huhtala.
† Princeton University.
‡ The University of Western Ontario.

10.1021/jp901228v CCC: $40.75
Published on Web 04/03/2009

properties of such aggregates,[17,18] for example, as nanocarriers in drug delivery.[9]

Our main findings can be summarized as follows. First, the presence of either type of excess salt leads to larger micellar aggregates than in their absence, in agreement with experimental observations. Second, the aggregate structures are markedly different in the cases of NaCl and $CaCl_2$. Specifically, the aggregates appear much more compact in the case of $CaCl_2$. The enhanced structural rigidity of the aggregates in the case of $CaCl_2$ is attributed to the formation of relatively long-lived (~0.5 ns) and stable salt bridges between nearest-neighbor head groups, mediated by the Ca^{2+} ions.

The rest of this paper is organized as follows. The next section is devoted to the description of the model, its parameters, and computational details. Then, in section 3 we summarize the results in terms of aggregate kinetics and structure in the presence of excess salt. Section 4 contains the discussion of our results, while concluding remarks are presented in section 5.

2. Methods

2.1. Computational Model. The Gromacs 3.3 simulation package[52−54] with the united atom parametrization was employed for the atomistic molecular dynamics (MD) simulations. The energies of the initial configurations were minimized with the steepest descent method. After the initialization, all simulations were performed in the *NpT* ensemble at $p = 1$ bar using the weak coupling method for pressure and temperature control.[55] The coupling times were set to 1.0 ps for pressure and 0.1 ps for temperature, and the temperatures of the solute, counterions, and solvent were controlled independently. The bond lengths of the detergent molecules were constrained by the LINCS algorithm[56] and those of the water molecules by SETTLE.[57] Time step of 2 fs was used in all of the simulations reported here. The Lennard-Jones interactions were cut off at 1 nm, and the full particle-mesh Ewald method[58] was employed for the long-ranged electrostatic interactions; not fully accounting for these long-ranged electrostatic interactions has been shown to lead to serious artifacts in the simulations of amphiphilic molecules,[59,60] and contrary to the rather common misconception, proper treatment of electrostatics is also computationally efficient.[61]

The SDS parameters are not part of the standard Gromacs force field. The parametrization employed in this work has been discussed and validated in detail in our previous work[37] and is available for download at http://www.softsimu.org/downloads.shtml. The sodium, calcium, and chloride ions were described by the Gromacs parameters; for a detailed discussion of ionic parameters, please see refs 62 and 63. The simple point charge (SPC) water model,[64] which is consistent with the chosen force field, was adopted for the water molecules. Visualizations of all molecular configurations were generated with VMD (visual molecular dynamics).[65] Since the micelle-forming systems studied here have typically multiple micelles, and micelle properties are computed for a given micelle, the data analysis relies on identifying to which micelle each SDS molecule belongs. The micelle classification scheme is based on geometrical distance constraints and has been described in detail in ref 37. Where applicable, the error has been estimated as the standard deviation of the data sample.

2.2. Simulated System. We have studied micellization of SDS molecules in the presence of two different types of excess salt (NaCl and $CaCl_2$). The number of SDS molecules in all simulations reported here was set to 400. Five extensive simulations (I−V), each 200 ns in duration while differing in the concentration and type of excess salt ions, were carried out. In these five simulations, I contained no excess salt, II contained additional 400 NaCl, III 1200 NaCl, IV 400 $CaCl_2$, and V 1200 $CaCl_2$ molecules. We note that an SDS molecule consists of an ionized Na^+ (the counterions which are released when SDS is immersed in an aqueous solution) and the anionic dodecylsulphate molecule, see Figure 1. Thus, even in the absence of excess salt, a solution of SDS contains free Na^+ counterions.

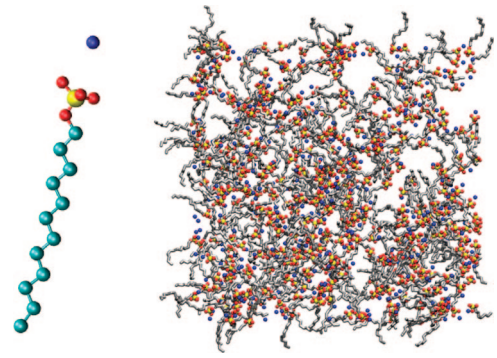

Figure 1. Left: The SDS molecule, where yellow represents sulfur, red oxygen, and light blue methyl group. The sodium counterion is displayed in blue. Right: An example of a random initial configuration of the 0.7 M 400 SDS-molecule system, here without excess salt. For clarity, the 25 371 water molecules are omitted from the visualization.

The simulated systems contained between 21 776 (the system with an excess of 1200 $CaCl_2$ molecules) and 25 371 (the system with no excess salt) water molecules; the number of water molecules varies between the systems because we desired to maintain the system volumes comparable in the simulations. In terms of concentrations, the above numbers correspond to an SDS concentration of 700 mM and NaCl/$CaCl_2$ concentration of 700 mM or 2.1 M in the ionic solutions.

Initially, the SDS molecules were placed randomly within the simulation box with the sodium counterions close to the SDS head groups, see Figure 1. After this, the simulation box was filled with water. In the simulations with excess salt, the ions were introduced by replacing randomly chosen water molecules. Subsequently, the total energy was minimized using the steepest descent algorithm. Temperature was maintained at 323 K. The temperature was deliberately chosen to be higher than the critical micellization temperature to facilitate aggregate formation. The first 30 ns of all the trajectories was considered as initial micelle formation period and was thus not included in the analysis. The remaining 170 ns was used for analysis. Specifically, although initial agglomeration takes place during the first 5 ns, see Figure 2, the micelle structure still evolves. Careful inspection of the micelle structural characteristics reveals that they have stabilized after 30 ns (data not shown), but we emphasize that the state represented between 30 and 200 ns is still evolving and is thus not an equilibrium state; final equilibration would take place on a time scale much longer than that achievable by current MD simulations. Having said that, the simulations reported here provide important molecular scale information about micelle structure and kinetics in the presence of excess salt.

3. Results

In the simulations, the initial SDS aggregation occurs rapidly, within the first few nanoseconds of the simulation. Figure 2 presents the aggregation numbers of the clusters as a function

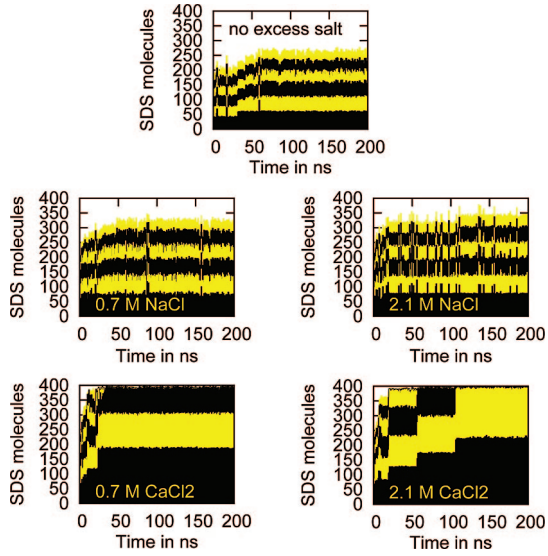

Figure 2. Micelle size distribution as a function of time. The cumulative size of the 6 largest micelles is plotted in the graphs. Occasionally, two micelles are classified as one if they are very close to one another, or one crystalline cluster is classified as two if the crystal has a stacking defect.

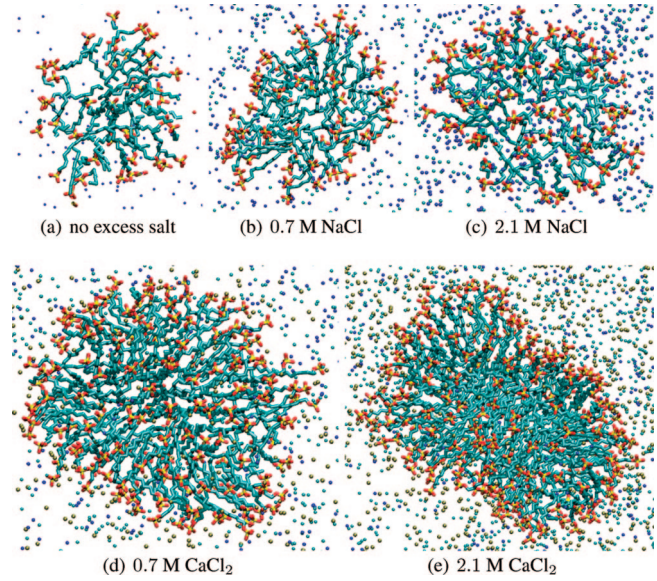

Figure 3. Examples of aggregate structures with and without excess ions. For each system, the largest micelle at the end of the simulation, i.e., at 200 ns, is presented. The spheres represent the ions (blue, sodium; cyan, chloride; tan, calcium) while surrounding micelles and water molecules have been omitted to facilitate visualization of the micelle.

of time. As expected, the presence of excess salt appears to drive the systems toward larger micelles which is in good agreement with experimental observations.[48] The effect is less prominent for excess NaCl than for $CaCl_2$, which is perhaps not surprising, since Ca^{2+} is a divalent ion and thus the resulting ionic strength of the solution is increased relative to NaCl. The excess ion type also affects aggregation dynamics: whereas micelles in the presence of excess NaCl undergo rapid fluctuations in size and shape, $CaCl_2$ reduces the magnitudes of fluctuations in both quantities; an implication of the latter is that the micellar aggregates appear more compact in the presence of $CaCl_2$ relative to the salt-free or excess NaCl systems. This deduction is confirmed by a visual inspection of the final configurations of the simulations presented in Figure 3: in the presence of the Na^+ counterions, or an excess of NaCl, the micelles appear disordered and fluctuate in shape, whereas the introduction of $CaCl_2$ drives the SDS to form more compact micelles with a smoother surface. It is interesting to note that there is little difference between the micellar structural characteristics of the 0.7 M and 2.1 M $CaCl_2$ systems. This can be attributed to the fact that even the smaller excess salt concentration is sufficient to provide an effective screening of the SDS headgroup charges. Furthermore, the Ca^{2+} ions participate in the formation of relatively long-lived salt bridges between the head groups. This will be discussed in more detail below.

3.1. Gauche Defects. To characterize the aforementioned structural changes we calculated the *gauche* defect probability of the hydrocarbon chains in the molecules. The data, shown in Figure 4, reveals that it is the excess ion type which impacts the *gauche* defect probability, while the probability depends only very weakly, if at all, on salt concentration. Specifically, the addition of excess NaCl does not affect the defect probability, while the presence of $CaCl_2$ results in a lower defect probability relative to the salt-free system due to more effective screening of repulsive head−head interactions. Interestingly, the defect probability is unaffected by changes in the $CaCl_2$ concentration at these elevated excess salt concentrations.

Another quantity closely related to the frequency of *gauche* defects in SDS molecules is their average length, defined as the linear separation between the sulfur atom and the C12-atom

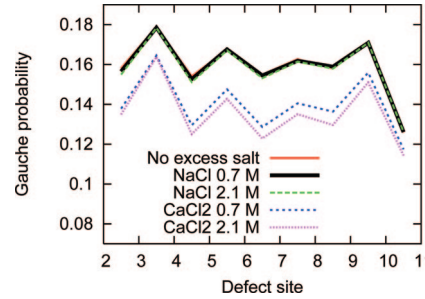

Figure 4. Gauche defect probability for different sites along the SDS hydrocarbon chain. The carbon site numbering starts from the C-atom next to the SO_4-headgroup and is plotted so that, for example, 2.5 refers to the bond between the second and third carbon atom in the chain. Nonpolar hydrogen atoms are treated as a compound with the neighboring carbon atom, and therefore, the horizontal axis ranges bonds from 2.5 to 10.5.

TABLE 1: Sodium Dodecyl Sulfate (SDS) Length *L*

system	L^a (nm)
no excess salt	1.36 ± 0.07
700 mM NaCl	1.35 ± 0.08
2.1 M NaCl	1.37 ± 0.06
700 mM $CaCl_2$	1.42 ± 0.01
2.1 M $CaCl_2$	1.46 ± 0.02

[a] The length is reported as the average S−C12 distance. Standard deviation was used to estimate the error.

at the end of the hydrocarbon chain. The data shown in Table 1 is in line with the *gauche* defect data: the monovalent sodium and chloride ions do not affect the length of the SDS molecule. However, the presence of divalent Ca^{2+} ions has a significant effect: the average SDS length has increased. In the presence of excess $CaCl_2$, the micelles are thus more compact with suppressed SDS conformational fluctuations, and undergo less severe shape fluctuations relative to the salt-free system and the ones with excess NaCl.

3.2. Ionic Charge Distribution. Let us next discuss the ionic charge distribution around the SDS head groups. Figure 5

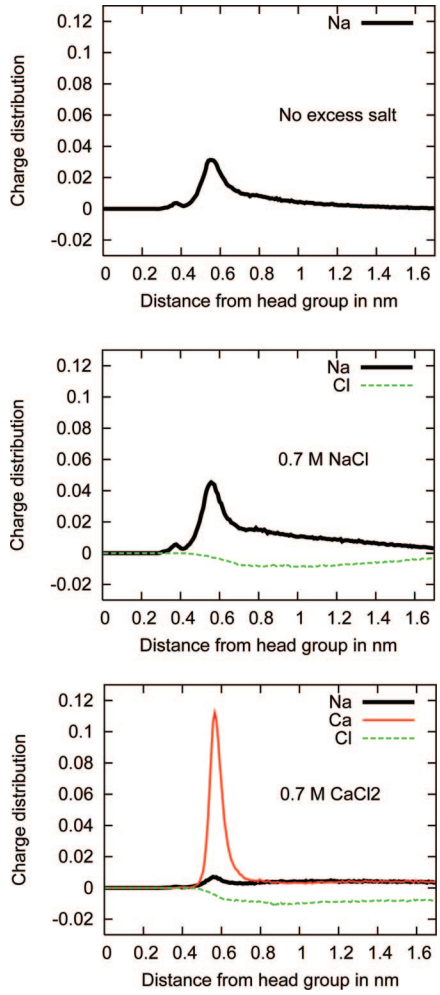

Figure 5. Charge distribution calculated as a function of distance to the S atom in the SDS headgroup.

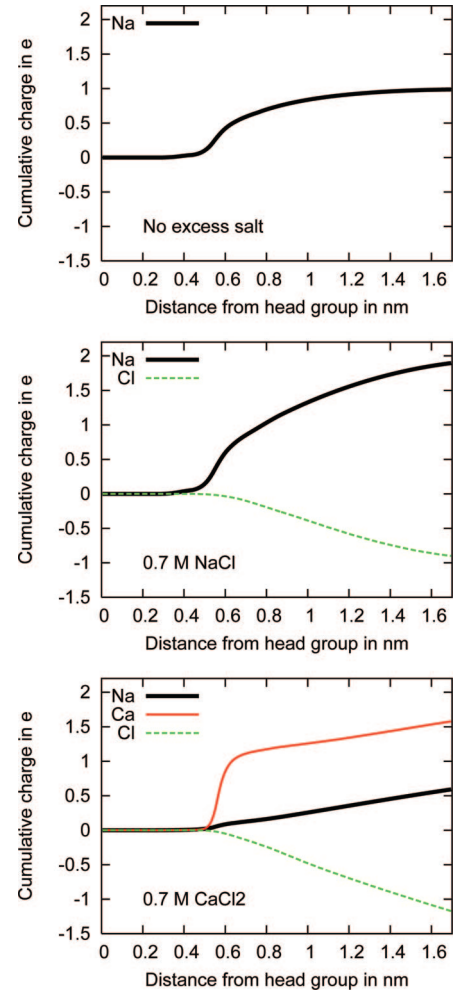

Figure 6. Componentwise contribution to the charge distribution calculated as a function of distance to the S atom in the SDS headgroup. The charge is calculated per headgroup. Note that the SDS headgroup has a total charge of −1.0 e.

displays the charge distribution measured as a function of the absolute radial distance from the SDS headgroup S atom for the salt-free and 700 mM excess NaCl or $CaCl_2$ systems; the behavior is similar in 2.1 M excess salt solutions. To minimize the effects of periodicity and influence of neighboring micelles in the analysis, a given ion contributes only to the charge distribution of the closest headgroup. Thus, we expect the resulting charge distributions to reflect those of widely separated micelles. The valency of the excess ion type has a very strong effect on the ionic charge distribution. In particular, the data clearly show that, when present, divalent Ca^{2+} ions dominate the behavior: they displace the Na^+ ions from the vicinity of the head groups almost entirely. Furthermore, the form of the Cl^- curves indicates the weak presence of an electric double layer, although the micellar surfaces are not well-defined. The small peak observed between 0.35 and 0.4 nm in the sodium curves in the salt-free or excess NaCl systems is associated with the first binding shell of the SDS model, as discussed in ref 37. The main Na^+ ion condensation peak is centered approximately at 0.58 nm and provides the dominant headgroup screening due to Na^+ ions, see ref 37. The cumulative charge distributions, shown in Figure 6, reveal the differences between the Na^+ and Ca^{2+} ions more clearly: the presence of Ca^{2+} gives rise to a much more rapid increase in charge density to screen the negatively charged SDS head groups relative to Na^+.

Whereas the preceding graphs describe the charge distributions componentwise, Figure 7 presents the total cumulative charge as a function of distance from the S atom in the SDS headgroup. Taking into account the polar characteristics of the water molecules, we observe that salt-free and excess NaCl systems are characterized by essentially identical charge distributions. On the other hand, a marked change is observed when $CaCl_2$ is introduced: $CaCl_2$ causes more rapid charge neutralization. That is, the first cumulative charge peak is lower than for the systems that have only sodium as the positive ion. On the other hand, systems with $CaCl_2$ exhibit several layers of charge; that is, more of the electric double layer can be observed especially at 2.1 M $CaCl_2$. Although the plot presenting the total charge including the polar water molecules does not show a difference between the salt-free and excess NaCl systems, a difference can be observed if the intrinsic charge distribution of water molecules is disregarded in the plot. As shown in the image on the right of Figure 7, additional Na^+ ions induce a more rapid neutralization of the headgroup charge. On the other hand, the presence of $CaCl_2$ causes an overshoot even after excluding the contribution of the water molecule orientation: recall that the SPC water model comprises a rigid three-body molecule with the hydrogens charged 0.41e while the oxygen has a charge −0.82e.[64] To correct the dipole moment, the hydrogen−oxygen−hydrogen angle is 109.47°. For the 2.1 M $CaCl_2$ even a minimum after the overshoot peak is observed again indicating some double layer formation.

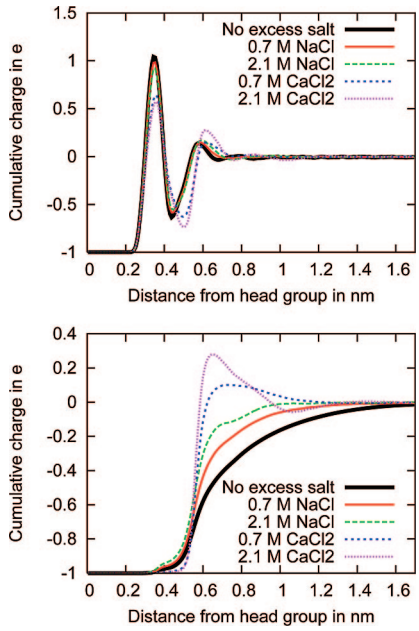

Figure 7. Top: Cumulative charge as a function of distance to the S atom in the SDS headgroup including the point charges of the solvent. Bottom: Cumulative charge distribution due to counterions and excess salt. Note that the SDS headgroup has a total charge of −1.0.

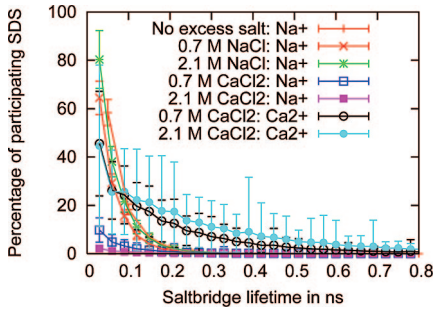

Figure 8. Probability of a salt bridge of given duration existing for any of the SDS head groups. The legend indicates the system and the ion mediating the salt bridge. Please note that, in the presence of excess $CaCl_2$, in addition to Ca^{2+} ions there are also the Na^+ counterions corresponding to the 0.7 M SDS concentration, and also, these may contribute to salt bridge formation.

3.3. Salt Bridges. Salt bridges[66,67] could be a plausible explanation for the structural difference between the micelles formed in solutions containing NaCl and $CaCl_2$. To study this aspect, we assessed the probability of a salt bridge of given duration existing between nearest-neighbor (NN) SDS headgroup pairs, see Figure 8.

A salt bridge was defined to exist when two headgroup S-atoms were bridged by a Na^+ or Ca^{2+} ion.[66,67] More specifically, if the same cation (Na^+ or Ca^{2+}) resides within a distance $R_{cut} = 0.72$ nm from two NN SDS head groups, a salt bridge is formed between the head groups. The specific value for R_{cut} is based on the radial distribution functions corresponding to Na^+ and Ca^{2+} condensation radii measured from the S-atoms in the headgroup. The same $R_{cut} = 0.72$ nm value corresponding to Ca^{2+} condensation radius was employed for both Na^+ and Ca^{2+} ions, although the respective ion condensation radius for Na^+ is 0.675 nm, see ref 37; this is justified as the outcome of the salt bridge analysis is only weakly sensitive to the employed R_{cut} value. Specifically, as long as R_{cut} is chosen such that only ions from the corresponding condensation shells contribute to salt bridges, the results are unchanged.

TABLE 2: Average Salt Bridge Lifetime

bridge ion	system	average lifetime (ns)
Na^+	no excess salt	0.08
Na^+	0.7 M NaCl	0.06
Na^+	2.1 M NaCl	0.07
Na^+	0.7 M $CaCl_2$	0.10
Ca^{2+}	0.7 M $CaCl_2$	0.21
Na^+	2.1 M $CaCl_2$	0.12
Ca^{2+}	2.1 M $CaCl_2$	0.30

Figure 8 shows that there are salt bridges in the system but their lifetimes are rather short, i.e., less than 1 ns. However, the probability distribution decays much faster for Na^+ mediated salt bridges than for Ca^{2+} mediated bridges; Ca^{2+} mediated salt bridges typically have significantly longer lifetimes. This is demonstrated by Table 2 which presents the average salt bridge lifetime for each system: Ca^{2+} mediated salt bridges are much more stable and have an average lifetime ($\leq$0.3 ns) that is significantly larger than that of Na^+ mediated ones ($\leq$0.1 ns). Furthermore, the presence of $CaCl_2$ stabilizes the Na^+ mediated bridges making their average lifetime longer. The stabilizing role of the Ca^{2+} mediated salt bridges can also be observed in the S−S shortest distance distribution, i.e., the NN distance distribution of the micelle head groups, shown in Figure 9. The data shows a sharper distribution peak for the $CaCl_2$ containing systems than for the systems with no excess salt or NaCl. Furthermore, the latter distributions are much broader in comparison to the $CaCl_2$ containing systems, implying the presence of larger structural fluctuations in the NaCl systems. Indeed, visual examination of the trajectories indicates that the dynamics of individual SDS species in the micelles is slower and more constrained in the presence $CaCl_2$. Additionally, the distributions presented in Figure 9 show a small shift in the peak position; that is, the most likely S−S NN distance is slightly smaller when $CaCl_2$ is introduced in comparison to the NaCl containing systems. This is to be expected as the greater screening strength of the Ca^{2+} ions should allow for denser packing of the head groups. However, with the studied concentrations, there is hardly any concentration dependence in the S−S NN distance distributions of the systems containing $CaCl_2$. This is due to the short screening length with $CaCl_2$; adding more $CaCl_2$ does not have a significant effect at small scales. However, the state of affairs is very different with small concentrations of NaCl: for the system with no excess salt and the two different concentrations of excess NaCl, the distribution can be seen to develop into a sharper peak as the concentration of NaCl is increased.

We conclude that Na^+ mediated salt bridges have such a short average lifetime that they are unlikely to contribute to the overall stability and structure of SDS micelles but for the Ca^{2+} ions the salt bridges may play a key role in stabilizing the micelles. The salt bridge analysis also shows that although the micelles are effectively screened by the ions, i.e., have very small effective charges, ion condensation is dynamic, i.e., the ions and head groups do not form permanent cation−anion pairs in the solution at $T = 323$ K.

It is interesting to note that we have observed strong indications of formation of rodlike micelles as the ionic strength of the solution increases. Specifically, at elevated salt concentrations, SDS molecules pack densely enough such that they effectively adopt a more cylindrical (rather than conelike) shape. It is well-known that a cylindrical packing volume favors rodlike micelles in comparison to spherical micelles, and thus, we conclude that an increase in the ionic strength eventually induces

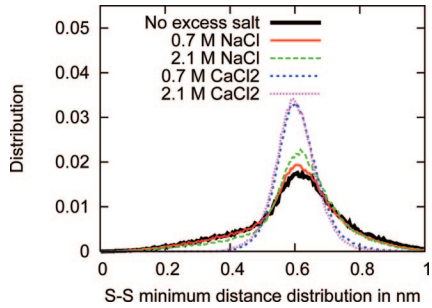

Figure 9. S−S nearest neighbor distance distribution.

a transition from spherical to elongated and finally to rodlike micelles. However, we are unable to probe this very interesting morphological transition regime at this point, as it is beyond the current capabilities of MD simulations.

4. Discussion

We have investigated the effect of monovalent and divalent ions on the formation of micellar aggregates using large-scale MD simulations with explicit solvent and salt. We observe salt bridges to play an important role in both stabilizing the micelles and increasing their size. Furthermore the presence of divalent Ca^{2+} ions is observed to dominate ion condensation around the micelles, leading to more compact aggregates in comparison with the monovalent Na^+.

In the 200 ns simulations performed in this work, we observe micelles with sizes from around 50 SDS to approximately 200 SDS depending on the amount and type of excess salt in the system. Additionally, we see indications of rodlike micellar structures as the ionic strength increases. Experimentally, it is well-established that the aggregation number of ionic micelles grows as a function of surfactant or ion concentration,[68−72] and our results fully agree with these observations. At critical micellization concentration (8 ± 1.4 mM, depending on measurement),[73−78] SDS forms micelles of size, i.e., aggregation number of 55−77 molecules[69,70,78,75,47] at temperatures close to the critical micellization temperature (CMT). Most of the measurements have been performed at temperatures closer to the CMT than in our simulations, in which the higher temperature facilitates more efficient exploration of micellization kinetics. The micelles we observe are significantly larger, potentially rodlike aggregates than in experiments without excess salt and the systems with excess salt.[79,80,70,72] It should also be noted that both the SDS and excess salt concentrations employed in this study are quite large, especially compared to the CMC. It is interesting to note that ref 79 reports that an increased temperature causes the SDS micelles asymptotically to approach a spherical shape with a hydrated radius of about 25 Å nearly independently of NaCl or SDS concentration. We are not aware of systematic data regarding SDS micelle size in the presence of multivalent ions at temperatures significantly above CMT. All in all, our observations are well in line with experimental observations: at the simulation temperature $T = 323$ K, we see almost spherical, slightly elongated micelles for the pure SDS solution and the systems with excess NaCl. Significant difference in the structure is only introduced with the divalent Ca^{2+} for which the micelles become visibly elongated with flat areas and areas of high curvature showing signs of potential transformation to rodlike structure. Furthermore, the simulation description restricts our observations: The micelles, once formed, are in a local energy minimum, and if the minimum is deep enough, it is unlikely that we see further size evolution within the sub-microsecond time window we are able to examine. Additionally, the enlarged micelles present at high SDS concentrations or in the presence of excess salt have been reported to be polydisperse in size which indicates a rather small free energy difference between the aggregate sizes.[3,81] We conclude that observed micelle sizes provide a lower limit to the actual micelle sizes in experiments.

Besides the size of the micelle, we observe the type of excess ions in the solution to influence the structure. In the presence of $CaCl_2$, Ca^{2+} replaces Na^+ as the condensed counterion, micelles are significantly more ordered and compact, and the surfactant molecules are effectively more rigid. Rigidity shows both in the dynamics and in the molecule length, or *gauche* defect probability. Ion interactions and their effects on dodecyl sulfate micelles have been studied in refs 35, 72, 79, and 82−87. The general agreement is that the ion type and concentration affect the micelle structure and dynamics. Particularly for dodecyl sulfate, ref 86 reports selective counterion condensation for sodium and lithium dodecyl sulfate in the presence of LiBr and NaBr; our observations of Ca^{2+} condensation dominance are well in line with these observations. Reference 35 provides a comparison between lithium, sodium, and ammonium counterions. Multivalent ions have been studied much less: The effects of Na^+, Ca^{2+}, and Al^{3+} on sodium dodecyl polyoxyethylene-2-sulfate micelles have been compared in ref 88 where even a small concentration of multivalent ions is reported to change the micelle shape and increase the aggregation number close to CMT. The observations are again well in line with our observations of excess Ca^{2+} inducing much more drastic changes in micelle structure, aggregation, and dynamics than excess Na^+. Additionally, Vasilescu et al.[87] report that an increasing Al^{3+} concentration first increases the SDS micelle size, and then causes precipitation, and when the Al^{3+} concentration is further increased, the precipitate becomes soluted again as wormlike micelles. This may happen with Ca^{2+} under proper conditions as well, and the observations of first an increase in the micelle size and then a transition to rodlike micelles are consistent with our results on Ca^{2+}, although we cannot conclude whether the micelles in our work are rodlike or elongated at high ionic concentrations.

In addition to studies of micelle interaction with various ions, there exist also studies of ion interactions with lipid bilayers.[89,90,67] Ion condensation, however, depends strongly on geometry.[91] Reference 89 reports that sodium ions affect both the structure and dynamics of a lipid bilayer. We observe a much smaller effect in the case of anionic micelles: SDS structure is hardly affected by the excess NaCl, but micellization dynamics becomes faster as the process is driven by the ions. Reference 90 shows that calcium becomes dominantly bound to lipid bilayers comprising POPC, and affects the structure. Our results agree with the observations: SDS micelles bind calcium strongly, and the structure of the micelles changes in the presence of the divalent ions. References 89 and 90 also claim a long relaxation time for the ions starting from the water phase with the presence of a preformed lipid bilayer. In our simulations, both the surfactants and ions form initially a random aqueous solution with the water molecules. As a result of this in our system the surfactant relaxation, i.e., reaching micelle structure equilibrium, is the bottleneck: we emphasize that the configurations analyzed in this work are metastable configurations.

It is tempting to compare our results with the Poisson−Boltzmann theory.[92,93] There is, however, a difficulty since it is not possible to uniquely determine the surface of a micelle as would be required by the theory. In addition, the surface is atomistic.

Strictly speaking, the Poisson−Boltzmann theory is valid only in the case of a smooth structureless surface. Such a fit has been performed, however, for a planar atomistic lipid bilayer by Gurtovenko et al.[94] Since it is easier to determine the surface plane for a bilayer, the authors were able to fit the charge distribution and compare with the Poisson−Boltzmann (or Gouy−Chapman, to be precise) theory in the case of a charged (cationic) lipid bilayer and no added salt. The simulation results and theory were in found to be in excellent agreement. With added salt, such as the case here, a different treatment is needed.[92,93]

Finally, in ref 67 ionic binding and Na^+ mediated ion bridges were demonstrated to play a key role in anionic lipid bilayers. This supports our finding of a large number of salt bridges in the ionic micelles, although we observe the Na^+ mediated bridges to be short, typically tens of picoseconds in duration. Ca^{2+}, however, forms salt bridges that are more stable and significantly longer in duration, hundreds of picoseconds, which makes these bridges a significant contribution to the micelle structure in the presence of Ca^{2+} ions.

5. Conclusions

In conclusion, we reported here the behavior of SDS micelles in the presence of excess NaCl or $CaCl_2$. The results show that salt, especially the divalent $CaCl_2$, can be used as a means to manipulate micelle properties. Specifically, our main findings can be summarized as follows. First, the presence of either excess salt leads to larger micellar aggregates than in its absence. Second, the aggregate structures are markedly different in the cases of NaCl and $CaCl_2$. For the latter, the aggregates appear much more compact. Third, the enhanced structural rigidity of the aggregates in the case of $CaCl_2$ arises from relatively long-lived (∼0.5 ns) salt bridges between nearest-neighbor head groups, mediated by the Ca^{2+} ions.

Acknowledgment. This work has been supported by the Natural Sciences and Engineering Research Council of Canada (M.K.), and through NSF-DMR Grant 0449184 (M.H.). We also thank the Southern Ontario SharcNet (www.sharcnet.ca) computing facility for computer resources.

References and Notes

(1) Hillmyer, M. A. *Science* **2007**, *317*, 604–605.
(2) Helenius, A.; Simons, K. *Biochim. Biophys. Acta* **1975**, *415*, 29–79.
(3) Zana, R. *Dynamics of Surfactant Self-Assemblies: Micelles, Microemulsions, Vesicles and Lyotropic Phases*; Vol. 126; CRC Press: Boca Raton, FL, 2005.
(4) Kékicheff, P.; Cabane, B. *J. Phys. (Paris)* **1987**, *48*, 1571–1583.
(5) Kékicheff, P.; Madelmont, G. C.; Ollivon, M. *J. Colloid Interface Sci.* **1989**, *131*, 112–132.
(6) Chernik, G. G. *Curr. Opin. Colloid Interface Sci.* **1999**, *4*, 381–390.
(7) Gradzielski, M. *Curr. Opin. Colloid Interface Sci.* **2004**, *9*, 256–263.
(8) Whitesides, G. M.; Grzybowski, B. *Science* **2002**, *295*, 2418–2421.
(9) Peer, D.; Karp, J. M.; Hong, S.; Farokhzad, O. C.; Margalit, R.; Langer, R. *Nat. Nanotechnol.* **2007**, *2*, 751–760.
(10) Torchilin, V. P. *Adv. Drug. Delivery Rev.* **2006**, *58*, 1532–1555.
(11) Bibette, J.; Calderon, F. L.; Poulin, P. *Rep. Prog. Phys.* **1999**, *62*, 969–1033.
(12) Anderson, B. C.; Cox, S. M.; Ambardekar, A. V.; Mallapragada, S. K. *J. Pharm. Sci.* **2001**, *91*, 180–188.
(13) Patist, A.; Kanicky, J. R.; Shukla, P. K.; Shah, D. O. *J. Colloid Interface Sci.* **2002**, *245*, 1–15.
(14) Rharbi, Y.; Winnik, M. A. *J. Am. Chem. Soc.* **2002**, *124*, 2082–2083.
(15) Rharbi, Y.; Winnik, M. A. *J. Phys. Chem. B* **2003**, *107*, 1491–1501.
(16) Rharbi, Y.; Chen, L.; Winnik, M. A. *J. Am. Chem. Soc.* **2004**, *126*, 6025–6034.
(17) Mohanty, A.; Patra, T.; Dey, J. *J. Phys. Chem. B* **2007**, *111*, 7155–7159.
(18) Renoncourt, A.; Vlachy, N.; Bauduin, P.; Drechsler, M.; Touraud, D.; Verbavatz, J. M.; Dubois, M.; Kunz, W.; Ninham, B. W. *Langmuir* **2007**, *23*, 2376–2381.
(19) Jusufi, A.; Hynninen, A.-P.; Haataja, M.; Panagiotopoulos, A. Accepted for publication in *J. Phys. Chem. B.* (2009).
(20) Larson, R. G. *J. Chem. Phys.* **1989**, *91*, 2479–2488.
(21) Larson, R. G. *J. Chem. Phys.* **1992**, *96*, 7904–7918.
(22) Dill, K. A.; Kopper, D. E.; Cantor, R. S.; Dill, J. D.; Bendedouch, D.; Chen, S. H. *Nature (London)* **1984**, *309*, 42–46.
(23) Dill, K. A.; Flory, P. J. *Proc. Natl. Acad. Sci.* **1981**, *78*, 676–680.
(24) Dill, K. A. *J. Phys. Chem.* **1982**, *86*, 1498–1500.
(25) Goetz, R.; Lipowsky, R. *J. Chem. Phys.* **1998**, *108*, 7397–7409.
(26) Bandyopadhyay, S.; Klein, M. L.; Martyna, G. J.; Tarek, M. *Mol. Phys.* **1998**, *95*, 377–384.
(27) Gao, J.; Ge, W.; Hu, G.; Li, J. *Langmuir* **2005**, *21*, 5223–5229.
(28) Cheong, D. W.; Panagiotopoulos, A. Z. *Langmuir* **2006**, *22*, 4076–4083.
(29) Drouffe, J. M.; Maggs, A. C.; Leibler, S. *Science* **1991**, *254*, 1353–1356.
(30) MacKerell, A. D. *J. Phys. Chem.* **1995**, *99*, 1846–1855.
(31) Tieleman, D. P.; van der Spoel, D.; Berendsen, H. J. C. *J. Phys. Chem. B* **2000**, 104.
(32) Marrink, S. J.; Tieleman, D. P.; Mark, A. E. *J. Phys. Chem. B* **2000**, *104*, 12165–12173.
(33) Bruce, C. D.; Senapati, S.; Berkowitz, M. L.; Perera, L.; Forbes, M. D. E. *J. Phys. Chem. B* **2002**, *106*, 10902–10907.
(34) Yamamoto, S.; Maruyama, Y.; Hyodo, S. A. *J. Chem. Phys.* **2002**, *116*, 5842–5849.
(35) Rakitin, A. R.; Pack, G. R. *J. Phys. Chem. B* **2004**, *108*, 2712–2716.
(36) Yakolev, D.; Boek, E. *Langmuir* **2007**, *23*, 6588–6597.
(37) Sammalkorpi, M.; Karttunen, M.; Haataja, M. *J. Phys. Chem. B* **2007**, *111*, 11722–11733.
(38) Sammalkorpi, M.; Karttunen, M.; Haataja, M. *J. Am. Chem. Soc.* **2008**, *130*, 17977–17980.
(39) Lazaridis, T.; Mallik, B.; Chen, Y. *J. Phys. Chem. B* **2005**, *109*, 15098–15106.
(40) Woods, M. C.; Haile, J. M.; O'Connell, J. P. *J. Phys. Chem.* **1986**, *90*, 1875–1885.
(41) Stephenson, B. C.; Beers, K.; Blankschtein, D. *Langmuir* **2006**, *22*, 1500–1513.
(42) Putnam, F. W.; Neurath, H. *J. Am. Chem. Soc.* **1944**, *66*, 692–697.
(43) Cabane, B. *J. Phys. (Paris)* **1981**, *42*, 847–859.
(44) Cabane, B.; Duplessix, R.; Zemb, T. *J. Phys. (Paris)* **1985**, *46*, 2161–2178.
(45) Mukerjee, P.; Mysels, K. J.; Kapauan, P. *J. Phys. Chem.* **1967**, *71*, 4166–4175.
(46) Aniansson, E. A. G.; Wall, S. N.; Almgren, M.; Hofmann, H.; Kielmann, I.; Ulbricht, W.; Zana, R.; Lang, J.; Tondre, C. *J. Phys. Chem.* **1976**, *80*, 905–922.
(47) Hayter, J. P.; Penfold, J. *Colloid Polym. Sci.* **1983**, *261*, 1022–1030.
(48) Berr, S. S.; Jones, R. R. M. *Langmuir* **1988**, *4*, 1247–1251.
(49) Aswal, V. K.; Goyal, P. S. *Phys. Rev. E* **2000**, *61*, 2947–2953.
(50) Dutt, G. B. *Langmuir* **2005**, *21*, 10391–10397.
(51) Zhang, J.; Ge, Z.; Jiang, X.; Hassan, P. A.; Liu, S. *J. Colloid Interface Sci.* **2007**, *316*, 796–802.
(52) Berendsen, H. J. C.; van der Spoel, D.; van Drunen, R. *Comput. Phys. Commun.* **1995**, *91*, 43–56.
(53) Lindahl, E.; Hess, B.; van der Spoel, D. *J. Mol. Model.* **2001**, *7*, 306–317.
(54) van der Spoel, D.; Lindahl, E.; Hess, B.; Groenhof, G.; Mark, A. E.; Berendsen, H. J. *J. Comput. Chem.* **2005**, *26*, 1701–1718.
(55) Berendsen, H. J. C.; Postma, J. P. M.; van Gunsteren, W. F.; Dinola, A.; Haak, J. R. *J. Chem. Phys.* **1984**, *81*, 3684–3690.
(56) Hess, B.; Bekker, H.; Berendsen, H. J. C.; Fraaije, J. G. E. M. *J. Comput. Chem.* **1997**, *18*, 1463–1472.
(57) Miyamoto, S.; Kollman, P. A. *J. Comput. Chem.* **1992**, *13*, 952–962.
(58) Essman, U.; Perela, L.; Berkowitz, M. L.; Darden, T.; Lee, H.; Pedersen, L. G. *J. Chem. Phys.* **1995**, *103*, 8577–8592.
(59) York, D. M.; Darden, T. A.; Pedersen, L. G. *J. Chem. Phys.* **1993**, *99*, 8345–8348.
(60) Patra, M.; Karttunen, M.; Hyvönen, M. T.; Falck, E.; Vattulainen, I. *J. Phys. Chem. B* **2004**, *108*, 4485–4494.
(61) Patra, M.; Hyvönen, M. T.; Falck, E.; Sabouri-Ghomi, M.; Vattulainen, I.; Karttunen, M. *Comput. Phys. Commun.* **2007**, *176*, 14–22.
(62) Patra, M.; Karttunen, M. *J. Comput. Chem.* **2004**, *25*, 678–689.

(63) Auffinger, P.; Cheatham, T. E.; Vaiana, A. C. *J. Chem. Theory Comput.* **2007**, *3*, 1851–1859.

(64) Berendsen, H. J. C.; Postma, J. P. M.; van Gunsteren, W. F.; Hermans, J. In *Intermolecular Forces*; Pullman, B., Ed.; Reidel: Dordrecht, 1981; pp 331−342.

(65) Humphrey, W.; Dalke, A.; Schulten, K. *J. Mol. Graphics* **1996**, *14*, 33–38.

(66) Murzyn, K.; Zhao, W.; Karttunen, M.; Kurdziel, M.; Róg, T. *Biointerphases* **2006**, *1*, 98–105.

(67) Zhao, W.; Rog, T.; Gurtovenko, A. A.; Vattulainen, I.; Karttunen, M. *Biophys. J.* **2007**, *92*, 1114–1124.

(68) Hall, D. G. *Langmuir* **1999**, *15*, 3483–3485.

(69) Croonen, Y.; Geladé, E.; van der Zegel, M.; van der Auweraer, M.; Vandendriessche, H.; de Scgryver, F. C.; Almgren, M. *J. Phys. Chem.* **1983**, *87*, 1426–1431.

(70) Quina, F. H.; Nassar, P. M.; Bonilha, P. M.; Bales, B. L. *J. Phys. Chem.* **1995**, *99*, 17028–17031.

(71) Bales, B. L.; Messina, L.; Vidal, A.; Peric, M.; Nascimiento, O. R. *J. Phys. Chem. B* **1998**, *102*, 10347–10358.

(72) Griffiths, P. C.; Paul, A.; Heenan, R. K.; Penfold, J.; Ranganathan, R.; Bales, B. L. *J. Phys. Chem. B* **2004**, *108*, 3810–3816.

(73) Esposito, C.; Colicchio, P.; Facchiano, A.; Ragone, R. *J. Colloid Interface Sci.* **1998**, *200*, 310–312.

(74) Gu, G.; Yan, H.; Chen, W.; Wang, W. *J. Colloid Interface Sci.* **1996**, *178*, 614–619.

(75) Johnson, I.; Olofsson, G.; Jönsson, B. *J. Chem. Soc., Faraday Trans. 1* **1987**, 83.

(76) Joshi, T.; Mata, J.; Bahadur, P. *Colloids Surf., A* **2005**, *260*, 209–215.

(77) Cifuentes, A.; Bernal, J.; Masa, D. J. C. *Anal. Chem.* **1997**, *69*, 4271–4274.

(78) Bastiat, G.; Grassl, B.; Khoukh, A.; Francois, J. *Langmuir* **2004**, *20*, 5759–5769.

(79) Mazer, N. A.; Benedek, G. B.; Carey, M. C. *J. Phys. Chem.* **1976**, *80*, 1075–1085.

(80) Llanos, P.; Zana, R. *J. Phys. Chem.* **1980**, *84*, 3339–3341.

(81) Siemiarczuk, A.; Ware, W. R. *J. Phys. Chem.* **1993**, *97*, 8082–8091.

(82) Lebedeva, N. V.; Shahine, A.; Bales, B. L. *J. Phys. Chem. B* **2005**, *109*, 19806–19816.

(83) Hayashi, S.; Ikeda, S. *J. Phys. Chem.* **1980**, *84*, 744–751.

(84) Srinivasan, V.; Blankschtein, D. *Langmuir* **2003**, *19*, 9932–9945.

(85) Tcacenco, C. M.; Zana, R.; Bales, B. L. *J. Phys. Chem. B* **2005**, *109*, 15997–16004.

(86) Aswal, V. K.; Goyal, P. S. *Phys. Rev. E* **2003**, *67*, 051401+.

(87) Vasilescu, M.; Angelescu, D.; Caldararu, H.; Almgren, M.; Khan, A. *Colloids Surf., A* **2004**, *235*, 57–64.

(88) Alargova, R.; Petkov, J.; Petsev, D.; Ivanov, I. B.; Broze, G.; Mehreteab, A. *Langmuir* **1995**, *11*, 1530–1536.

(89) Böckmann, R. A.; Hac, A.; Heimburg, T.; Grubmüller, H. *Biophys. J.* **2003**, *85*, 1647–1655.

(90) Böckmann, R. A.; Grubmüller, H. *Angew. Chem., Int. Ed.* **2004**, *43*, 1021–1024.

(91) Netz, R. R. *J. Phys.: Condens. Matter* **2004**, *16*, S2353–S2368.

(92) Oosawa, F. *Polyelectrolytes*; Marcel Dekker Inc.: New York, 1971..

(93) Lamm, G. *Rev. Comput. Chem.* **2003**, *19*, 147–365.

(94) Gurtovenko, A. A.; Miettinen, M.; Karttunen, M.; Vattulainen, I. *J. Phys. Chem. B* **2005**, *109*, 21126–21134.

JP901228V